JOC The Journal of Organic Chemistry

Article

pubs.acs.org/joc

NMR Spectroscopic Characterization and DFT Calculations of Zirconium(IV)-3,3′-Br_2−BINOLate and Related Complexes Used in an Enantioselective Friedel−Crafts Alkylation of Indoles with α,β-Unsaturated Ketones

Gonzalo Blay,[†] Joan Cano,*[,‡] Luz Cardona,[†] Isabel Fernández,[†] M. Carmen Muñoz,[§] José R. Pedro,*[,†] and Carlos Vila[†]

[†]Departament de Química Orgànica, Facultat de Química, Universitat de València, Dr. Moliner 50, E-46100-Burjassot, València, Spain

[‡]Institut de Ciència Molecular (ICMol), Universitat de València, and Fundació General de la Universitat de València (FGUV), E-46980 Paterna, València, Spain

[§]Departament de Física Aplicada, Universitat Politècnica de València, Camí de Vera s/n, E-46022 València, Spain

Supporting Information

ABSTRACT: Experimental and theoretical studies on the structure of several complexes based on (*R*)-3,3′-Br_2−BINOL ligand and group (IV) metals used as catalysts in an enantioselective Friedel−Crafts alkylation of indoles with α,β-unsaturated ketones have been carried out. NMR spectroscopic studies of these catalysts have been performed, which suggested that at room temperature the catalysts would form a monomeric structure in the case of Ti^{IV} and a dimeric structure in the cases of Zr^{IV} and Hf^{IV}. Density functional theory (DFT) calculations clearly corroborate the conclusions of these experimental spectroscopic studies. The dimeric structure with a doubly bridged motif [Zr^{IV}_2(μ-(*R*)-3,3′-Br_2−BINOL)$_2$] where each binaphthol ligand acts as bridge between the metal centers (Novak's model) is more stable than the dimeric structure with a doubly bridged motif [Zr^{IV}_2(μ-O^{t}Bu)$_2$] where the *tert*-butoxide groups act as bridging ligands (Kobayashi's model). The scope of the Friedel−Crafts alkylation with regard to the indole structure has been studied. Finally a plausible mechanism for the Friedel−Crafts reaction and a stereomodel for the mode of action of the catalyst that explain the observed stereochemistry of the reaction products have been proposed.

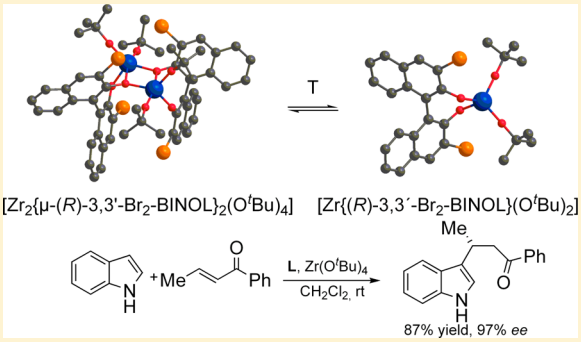

INTRODUCTION

Development of synthetic procedures that allow the preparation of enantiomerically pure or enriched products has attracted much attention in the past decades[1] due to the importance of the absolute stereochemistry of the molecules on their biological activity[2] as well as on the properties of materials.[3] In this context, asymmetric catalysis based on metal complexes is one of the most important synthetic approaches to chiral nonracemic products. In fact considerable progress on the development of catalytic enantioselective procedures has been achieved in the past decade. The 1,1′-binaphthyl-2,2′-diol (BINOL) scaffold has been extensively used to control many asymmetric processes having demonstrated high chiral discrimination properties[4] in a great number of enantioselective processes. Group (IV) metal ions, mainly titanium and in minor extension zirconium and hafnium, have been used with BINOL derivatives, because the catalysts are easily generated in situ and the metal-containing starting materials are commercially available. Additionally, group (IV) metals form strong bonds to oxygen, resulting in stabilization of the (BINOLate)−metal moiety. On the other hand the Lewis acidity of these (BINOLate)MX_2 (M= Ti, Zr, Hf; X= ligand) complexes can be easily tuned by variation of the electronic properties of the X ligands and influenced by the substituent at 3,3′ and 6,6′ positions of the BINOL scaffold.[5]

A huge number of highly enantioselective synthetic procedures employing titanium−BINOL derived catalysts have been developed by different authors.[6] Furthermore, several zirconium−BINOL derived catalysts have been developed by Kobayashi and other authors that have been utilized in highly enantioselective processes, such as Mannich-type reactions,[7] hetero-Diels−Alder cycloadditions,[8] [3 + 2] cycloadditions,[9] Strecker reactions,[10] allylation of imines,[11] Mukaiyama aldol condensation,[12] meso-aziridine ring-opening reactions,[13] allylation of aldehydes,[14] aldol reactions,[15] and aldol-Tishchenko reactions.[16] Also a hafnium−BINOL complex has been developed by Kobayashi and used in an

Received: July 2, 2012
Published: November 5, 2012

enantioselective Mannich-type reaction.[17] Recently we have shown that $Zr(O^tBu)_4$–BINOL complexes are very effective catalysts for the enantioselective Friedel–Crafts alkylation of indoles with α,β-unsaturated ketones.[18]

However, in spite of the versatility and enantioselectivity of the titanium or zirconium–BINOL-based catalysts, investigations into the structure of these species and their reaction mechanisms have been scarce. The kinetic lability of group (IV) metal alkoxides, the Lewis acidic nature of the metal center, the variable coordination geometries and the strong tendency to produce equilibrium mixtures of polynuclear oligomers make the task of identifying the actual molecular species participating in the different chemical processes extremely difficult.[19]

Studies in solution as well as in solid-state of the complexes generated from BINOL derivatives with titanium alkoxides that are relevant to our investigation have been reported. Heppert[20] found that 3,3′-disubstituted binaphthols (3,3′-R_2–BINOL) produced monomeric complex [Ti(3,3′-R_2–BINOLate)$(O^iPr)_2$] when R was very large [R = Si(^{t}Bu)Me_2]. In contrast, when the 3,3′-substituents were methyl groups, a dimeric complex was obtained, which consisted of a double bridged motif [$Ti^{IV}_2(\mu$-3,3′-R_2–BINOL$)_2$] where each binaphthol ligand acts as bridge between the metal centers. Novak[21] synthesized several chiral binaphthyl titanium alkoxide complexes, among which the titanium complex [Ti{(*R*)-3,3′-Br_2–BINOLate}$(O^tBu)_2]_n$ has a structure in solid state similar to the dimer described by Heppert [Ti_2{(*R*)-3,3′-Me_2–BINOLate$}_2(O^iPr)_4$], although in solution at room temperature presents a monomeric structure. On the other hand, Kobayashi[22] prepared a new complex from $Zr(O^tBu)_4$ and (*R*)-3,3′-I_2–BINOL in presence of *n*-propanol and water. The author suggested that this complex has a dimeric structure with a doubly bridged motif [$Zr^{IV}_2(\mu$–OH$)$ (μ-O^{n}Pr)] where the hydroxyl and the *n*-propoxide act as bridging ligands.

RESULTS AND DISCUSSION

As a part of our research on asymmetric catalysis using chiral Lewis acids, we have previously reported the enantioselective Friedel–Crafts alkylation of indoles with α,β-unsaturated ketones (Scheme 1).[18] The best results were obtained by using a complex formed from equimolar amounts of (*R*)-3,3′-Br_2–BINOL and $Zr(O^tBu)_4$ in dichloromethane, which allowed us to obtain the desired products with good yields and enantiomeric excesses above 95% in most of the studied examples (see below). To gain insight about the structure of the catalytic species involved and the mechanism of the reaction, we have performed a detailed structural study using a double approach involving both ^{1}H and ^{13}C NMR spectroscopic measures and theoretical study by density functional theory (DFT), including the study of the corresponding titanium and hafnium complexes with comparative purposes. Attempts to determine the exact molecular mass of the generated complexes using soft-ionization techniques (ESI) were unsuccessful, probably because the ionizing solvents required for this technique alter the complex structure.[23] We have also enlarged the study of the scope of the reaction, particularly with regard to the structure of the indole partner, which is relevant to make a proposal of the mechanism of the reaction.

Scheme 1. Friedel–Crafts Reaction of Indoles with α,β-Unsaturated Ketones and Structure of (*R*)-3,3′-Br_2–BINOL Used in This Study

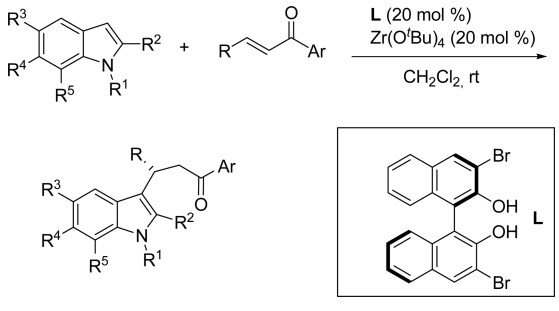

NMR Spectroscopic Characterization of the Complexes. For the ^{1}H and ^{13}C NMR spectroscopic analysis, the metal complexes were generated in situ from stoichiometric quantities of (*R*)-3,3′-Br_2–BINOL (**L**) and the corresponding metal *tert*-butoxides in CD_2Cl_2 at room temperature under identical conditions as in the enantioselective reaction. Figure 1a–d shows the aromatic region of the ^{1}H NMR spectra for the free (*R*)-3,3′-Br_2–BINOL (**L**) (a) and the Ti$(O^tBu)_4$-(*R*)-3,3′-Br_2–BINOL (b), $Zr(O^tBu)_4$-(*R*)-3,3′-Br_2–BINOL (c) and Hf$(O^tBu)_4$-(*R*)-3,3′-Br_2–BINOL (d) complexes, respectively, measured at room temperature. Figure 2a–d shows the aromatic region of the corresponding ^{13}C NMR spectra. It is important to note that under these conditions, the signals of the free (*R*)-3,3′-Br_2–BINOL completely disappeared and a new set of resonances with different chemical shift was observed.

In the case of the complex formed from Ti$(O^tBu)_4$ and (*R*)-3,3′-Br_2–BINOL the ^{1}H NMR (Figure 1b) and the ^{13}C NMR (Figure 2b) spectra show a single set of resonances for the 3,3′-Br_2–BINOLate ligand (without splitting of the signals). The upfield region of the ^{1}H spectrum includes, besides the singlet that corresponds to the free *tert*-BuOH,[24] a singlet corresponding to two magnetically equivalent O^{t}Bu moieties at 1.06 ppm. Table 1 lists the ^{1}H NMR assignments for the ligand **L** as well as for the complexes (data for the ^{13}C NMR spectrum appear in the Experimental Section). It is interesting to note the upfield shifts that are produced after binding of the 3,3′-Br_2–BINOL ligand to the metal center. These simple ^{1}H NMR and ^{13}C NMR spectra (without splitting of the signals) imply a structure with C_2-symmetry, which indicates that the complex exists as a monomer (Figure 3). This interpretation is in accordance with the results obtained by Novak[21] for the same compound in solution at room temperature, in spite of the structure obtained by diffraction of X-ray at low temperature, which indicated that the complex is a dimer in solid state. On the other hand, in his work about the structure of a related complex prepared from (*R*)-3,3′-Me_2–BINOL and Ti$(O^iPr)_4$, Heppert[20] obtained also a simple ^{1}H NMR spectrum (without splitting of the signals), which would imply a C_2-symmetric species. However, this author proposed that the simplicity in the ^{1}H NMR might arise from a [Ti_2{(*R*)-3,3′-Me_2–BINOL$}_2(O^iPr)_4$] dimer undergoing an intramolecular exchange of (*R*)-3,3′-Me_2–BINOLate via cleavage of one bond between each titanium and bridging oxygen. For our complex prepared from (*R*)-3,3′-Br_2–BINOL and Ti$(O^tBu)_4$, we believe the monomeric structure in solution to be more likely, since the complexes prepared from either racemic or optically pure (*R*)-3,3′-Br_2–BINOL gave undistinguishable ^{1}H NMR and ^{13}C NMR spectra at room temperature. As we will see below, DFT calculations corroborate that the complex formed from (*R*)-3,3′-Br_2–BINOL and Ti$(O^tBu)_4$ has a monomeric structure at room temperature.

dx.doi.org/10.1021/jo3013594 | J. Org. Chem. 2012, 77, 10545–10556

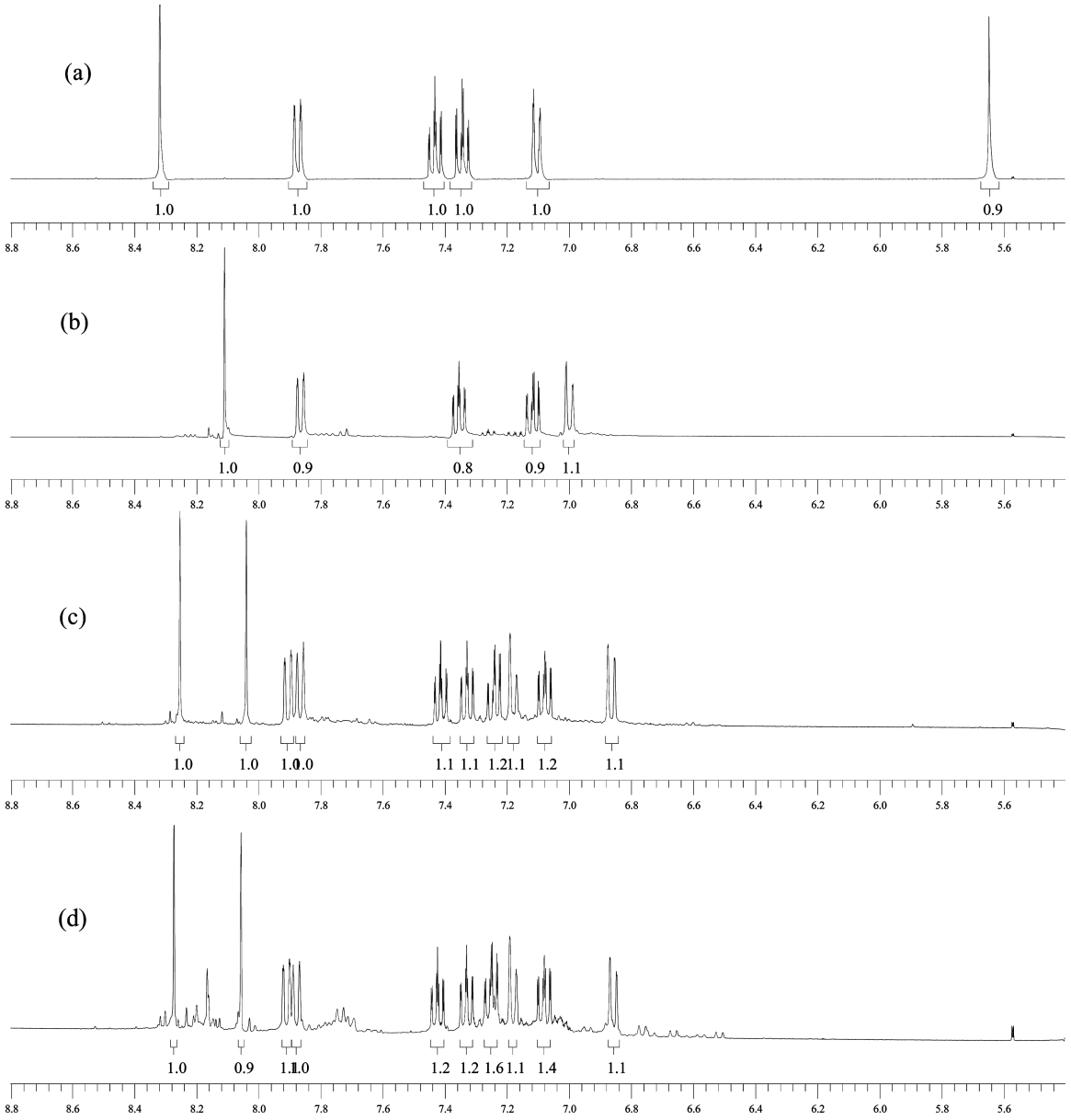

Figure 1. Aromatic region of the ^{1}H NMR spectra of (a) (*R*)-3,3′-Br_2−BINOL (**L**), (b) Ti(O^tBu)$_4$-(*R*)-3,3′-Br_2−BINOL, (c) Zr(O^tBu)$_4$-(*R*)-3,3′-Br_2−BINOL, (d) Hf(O^tBu)$_4$-(*R*)-3,3′-Br_2−BINOL in CD_2Cl_2 at 298 K.

On the other hand, the complexes formed from the same ligand (*R*)-3,3′-Br_2−BINOL and Zr(O^tBu)$_4$ or Hf(O^tBu)$_4$ showed completely different spectroscopic features to those with Ti(O^tBu)$_4$. Thus, the ^{1}H NMR (Figure 1c,d) and ^{13}C NMR (Figure 2c,d) spectra for these complexes showed a splitting of all resonances; that is, the aromatic region of the ^{1}H NMR spectra showed 10 well-resolved signals, and the ^{13}C NMR spectra showed 20 signals corresponding to the binaphthyl groups. Both spectra indicated that the C_2-symmetry of the 3,3′-Br_2−BINOLate ligand had been lost. Besides the resonance at δ 1.26 ppm that corresponds to the free ^{t}BuOH, characteristic singlets of the bound *tert*-butoxide at δ 0.95 and 0.96 ppm for the zirconium complex (δ 0.94 and 0.95 ppm for the hafnium complex), were also observed. The integration of the signals in the ^{1}H NMR spectrum indicated that there are two bound *tert*-butoxides for every 3,3′-Br_2−BINOL ligand. The unequivalence of the naphtholate and *tert*-butoxide ligands is consistent with the existence of a dimeric structure[20] with C_2 symmetry [Zr_2{(*R*)-3,3′-Br_2−BINOL}$_2$(O^tBu)$_4$] and [Hf_2{(*R*)-3,3′-Br_2−BINOL}$_2$(O^tBu)$_4$], in which the two metal ions are joined by means of aryloxide, [M^{IV}_2{μ-(*R*)-3,3′-Br_2−BINOL}$_2$] (Novak's model), or alkoxide, [M^{IV}_2(μ-O^tBu)$_2$] bridges (Kobayashi's model) (Figure 4). As we will discuss later, DFT calculations corroborate that these complexes of zirconium and hafnium have a dimeric structure at room temperature.

Next, we performed ^{1}H NMR spectroscopic measures at variable temperature. Previous experiments with the complex prepared from (*R*)-3,3′-Br_2−BINOL and Ti(O^tBu)$_4$ have been reported by Novak.[21] This author found that when the temperature was lowered, the well-resolved resonances observed at room temperature were broadened at 223 K to give new resonance peaks below 213 K. These results were interpreted as the complex existing as a monomer above 223 K but as monomer and dimer mixture below 203 K. In our study with the same complex in CD_2Cl_2 (see Supporting

dx.doi.org/10.1021/jo3013594 | J. Org. Chem. 2012, 77, 10545−10556

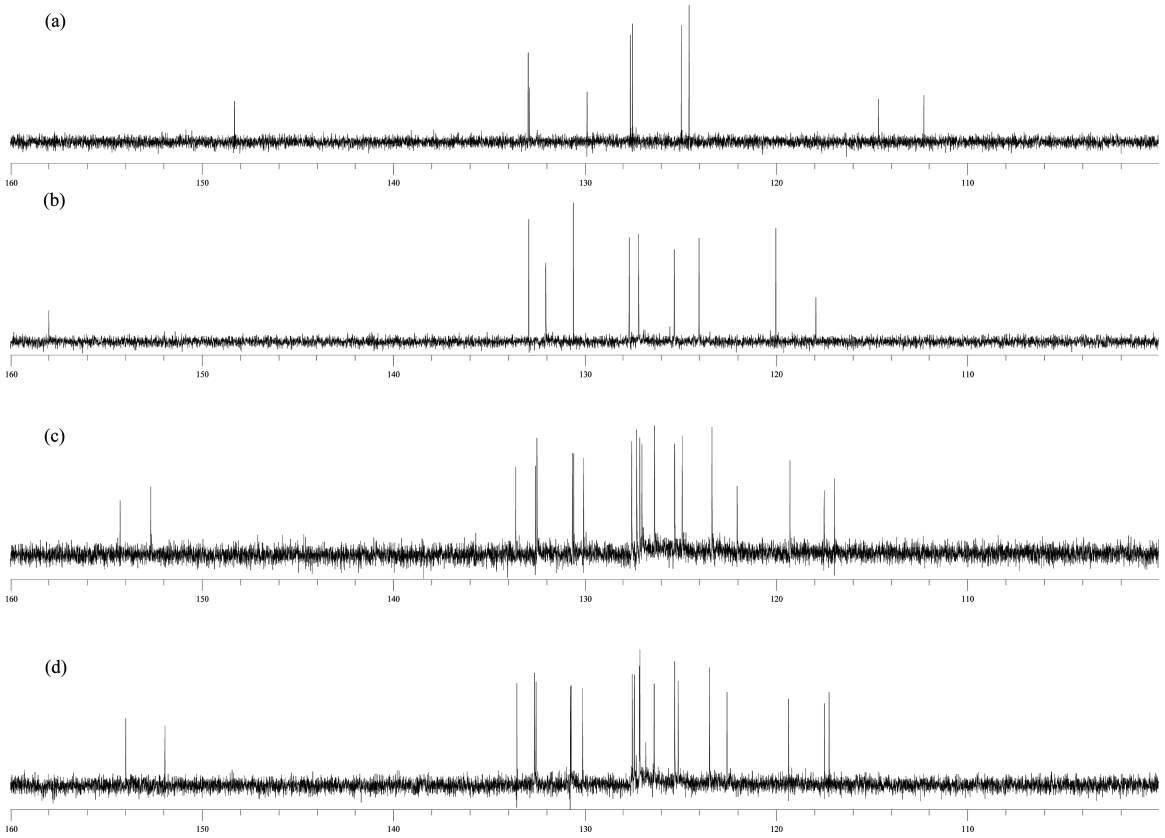

Figure 2. Aromatic region of the ^{13}C NMR spectra of (a) (*R*)-3,3′-Br_2−BINOL (**L**), (b) Ti(O^tBu)$_4$-(*R*)-3,3′-Br_2−BINOL, (c) Zr(O^tBu)$_4$-(*R*)-3,3′-Br_2−BINOL, (d) Hf(O^tBu)$_4$-(*R*)-3,3′-Br_2−BINOL in CD_2Cl_2 at 298 K.

Table 1. ^1H NMR Assignments for the Complexes of Ti, Zr, and Hf in CD_2Cl_2 at Room Temperature

sample	H4	H4′	H5	H5′	H6	H6′	H7	H7′	H8	H8′	OH	^{t}BuOH	^{t}BuO	^{t}BuO′
L	8.32	–	7.88	–	7.43	–	7.35	–	7.11	–	5.65	–	–	–
L-Ti(O^tBu)$_4$	8.11	–	7.87	–	7.36	–	7.12	–	7.00	–	–	1.26	–	1.06
L-Zr(O^tBu)$_4$	8.25	8.04	7.87	7.90	7.41	7.33	7.22	7.08	7.18	6.86	–	1.26	0.96	0.95
L-Hf(O^tBu)$_4$	8.27	8.06	7.88	7.91	7.42	7.33	7.25	7.08	7.18	6.86	–	1.25	0.95	0.94

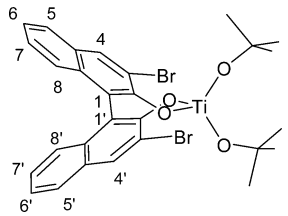

Figure 3. Structure for the monomer [Ti{(*R*)-3,3′-Br_2−BINOL}-(O^tBu)$_2$].

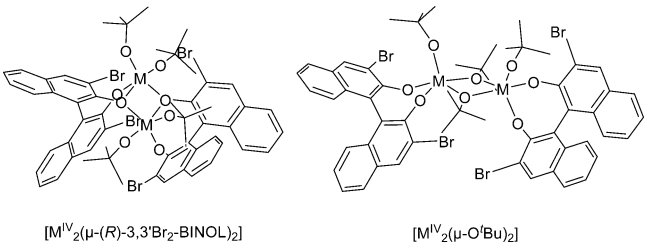

Figure 4. Models for the dinuclear [M_2\{(*R*)-3,3′-Br_2−BINOL\}$_2$(O^tBu)$_4$] complexes.

Information), we found that the same set of well-resolved resonances observed at room temperature was kept unaltered at 273 and 253 K. At 223 K each of the resonances in the spectrum was broadened, undergoing decoalescence to produce a pair of signals at 203 K. The clear split of the resonances as well as their relative integration suggest to us that, at this low temperature, the complex exists as a dimer rather than a monomer and dimer mixture as interpreted by Novak. The spectroscopic behavior of our complex is quite similar to that described by Heppert for the related complex Ti(O^iPr)$_4$-(*R*)-3,3′-Me_2−BINOL in toluene, the temperature of decoalescence (193 K) being the only difference, although this author interpreted that his complex is a dimer at room temperature and this decoalescence is due to a slow ligand exchange instead of a monomer−dimer transformation.

On the other hand, ^1H NMR spectra of the complexes formed from equimolar amounts of ligand (*R*)-3,3′-Br_2−BINOL (**L**) and Zr(O^tBu)$_4$ or Hf(O^tBu)$_4$ (see Supporting Information) remained unaltered between 303 and 223 K, indicating that their structure does not change significatively in this temperature range. As mentioned earlier, the unequivalence of the resonances corresponding to the protons of the naphthalene rings and the *tert*-butoxide ligands indicates that

dx.doi.org/10.1021/jo3013594 | J. Org. Chem. 2012, 77, 10545−10556

the complexes maintain the structure of dimer with C_2 symmetry in the temperature range studied. In these dimers, the two metal ions are joined by means of aryloxide or alkoxide bridges and they should adopt an edge-fused bis-trigonal-bipyramidal coordination environment,[20] such as Heppert proposed for the $[Ti_2\{(R)\text{-}3,3'\text{-}Me_2\text{–}BINOL\}_2(O^iPr)_4]$ dimer at low temperatures.

On the view of the different temperature-dependent behavior showed by the Ti, Zr and Hf complexes and the different interpretations of this behavior for the titanium complexes, we decided to carry out a theoretical study for the monomer–dimer interconversion.

Optimization of the Molecular Geometry by Using DFT Calculations. Density functional theory (DFT) calculations have been performed in order to understand the observed experimental differences in the temperature-dependent mononuclear/dinuclear solution equilibrium for the titanium(IV) and zirconium(IV) systems (see Computational Details in the Experimental Section).[25−30] Despite the limitations of these kinds of calculations to study the large number of possible molecules that may exist in solution, they can help to discard or validate them. The optimized geometries for the mononuclear and dinuclear complexes are shown in Figures 5 and 6, respectively. Two different geometries of the dinuclear complexes have been considered. The first model is based on the X-ray crystal structure of the dititanium(IV) complex reported by Novak,[21] which consists of a doubly bridged motif $[M^{IV}_2\{\mu\text{-}(R)\text{-}3,3'\text{-}Br_2\text{–}BINOL\}_2]$ where each (R)-3,3′-Br_2–BINOL ligand acts as bridge between the metal centers. The second model consists of a doubly bridged motif $[M^{IV}_2(\mu\text{-}O^tBu)_2]$ where the *tert*-butoxide groups act as bridging ligands, as proposed by Kobayashi for the structure of the dizirconium(IV) complex.[22] In this case, different dispositions of the peripheral ligands, allowing or not the presence of weak carbon-based hydrogen-bonds,[31] have been also considered in the energy calculations in order to find the most stable ones. Although other possible geometries and molecules can be envisaged, those studied here seem the most logical from the spectroscopic study and, moreover, they have allowed the understanding of the experimental results, as it will be shown below.

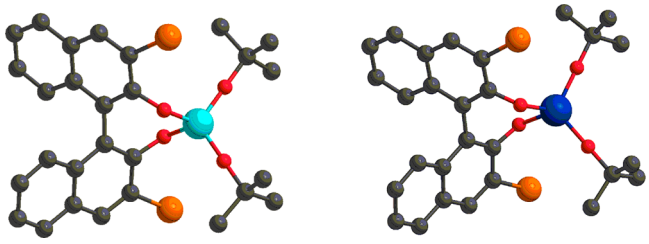

Figure 5. Optimized geometries for the mononuclear $[Ti\{(R)\text{-}3,3'\text{-}Br_2\text{–}BINOL\}(O^tBu)_2]$ and $[Zr\{(R)\text{-}3,3'\text{-}Br_2\text{–}BINOL\}(O^tBu)_2]$ complexes. Carbon, oxygen, bromide, titanium and zirconium atoms are shown in gray, red, brown, light blue and dark blue, respectively. Hydrogen atoms are not displayed to make visualization easier.

The DFT energy calculations show that the Novak's dinuclear model is more stable than the Kobayashi's one for both the titanium(IV) and zirconium(IV) compounds. Otherwise, a rather good agreement between the calculated and experimental geometries is observed for the titanium(IV) compound, in terms of both bond distances and angles (Figure 7). The largest deviations are observed for the calculated metal–ligand distances, which are greater than the experimental ones, as it is commonly found in geometry optimization calculations of first transition metal complexes using the B3LYP functional.

The calculated values of the stabilization energy (ΔE), defined as the difference between the electronic energy of the optimized dinuclear and mononuclear species ($\Delta E = E^{din} - 2E^{mon}$), are −14.1 and −40.7 kcal/mol in the titanium(IV) and zirconium(IV) compounds, respectively. These negative values show that the dinuclear compound is more stable. Overall, the theoretical results agree with the experimental ones, which show that the dinuclear complex is the only species present in solution at 220 K for both the titanium(IV) and zirconium(IV) systems. It must be stressed, however, that the calculated E^i values are not the real ones, but they correspond to the energy minimum of the molecule. Strictly speaking, the stabilization energy should be calculated from the energy of the first vibrational state, so-called zero-point energy (E^i0). That being so, we have performed additional vibrational frequency calculations for both the mono- and dinuclear molecules. The corrected ΔE values are then −12.2 and −39.0 kcal/mol for the titanium(IV) and zirconium(IV) systems, respectively, and still predict a more stable dinuclear form in both cases.

On the other hand, the enthalpic and entropic contributions to the free energy can be determined with the aid of the vibrational frequency calculations, thus allowing us to evaluate the influence of the temperature on the mononuclear/dinuclear equilibrium for these systems. In a first approximation, the free energy calculations have been carried out for an ideal gas situation. The enthalpy and entropy have been determined at each temperature from the electronic, vibrational, rotational, and translational energy contributions. The calculated free energy variation (ΔG), defined as the difference between the free energy of the optimized dinuclear and mononuclear species ($\Delta G = G^{din} - 2G^{mon}$), is related to the equilibrium constant of the dimerization reaction (K) through $\Delta G = -RT \ln K$. The temperature dependence of the dinuclear concentration can then be calculated for both the titanium(IV) and zirconium(IV) systems (Figure 8). For a zero value, the dinuclear complex is not present at all in solution, while the unity value is proposed when only the dinuclear complex exists in solution. The temperature that separates the regions where mononuclear or dinuclear complexes are predominant is indicated with a vertical gray line. In each region is included a picture of molecular geometry of the prevalent complex.

The calculated distribution diagram for the titanium(IV) system indicates that the dinuclear complex is the major species below 180 K. Above 180 K, the dinuclear complex dissociates to give two mononuclear complexes, in agreement with the experimental results based on the ^{1}H NMR studies in solution. The vibrational and rotational energy contributions are the main factors responsible for the stabilization of the mononuclear complex at room temperature. Contrarily, the calculated distribution diagram for the zirconium(IV) system indicates that the dinuclear complex is the unique species up to room temperature, in agreement with the experimental results based on the ^{1}H NMR studies in solution. This situation results from the greater absolute value of ΔE for the zirconium(IV) compound compared with that for the titanium(IV) one, which is explained by the larger steric hindrance between the 3,3′-Br_2–BINOL and *tert*-butoxide ligands in the latter because of

dx.doi.org/10.1021/jo3013594 | J. Org. Chem. 2012, 77, 10545−10556

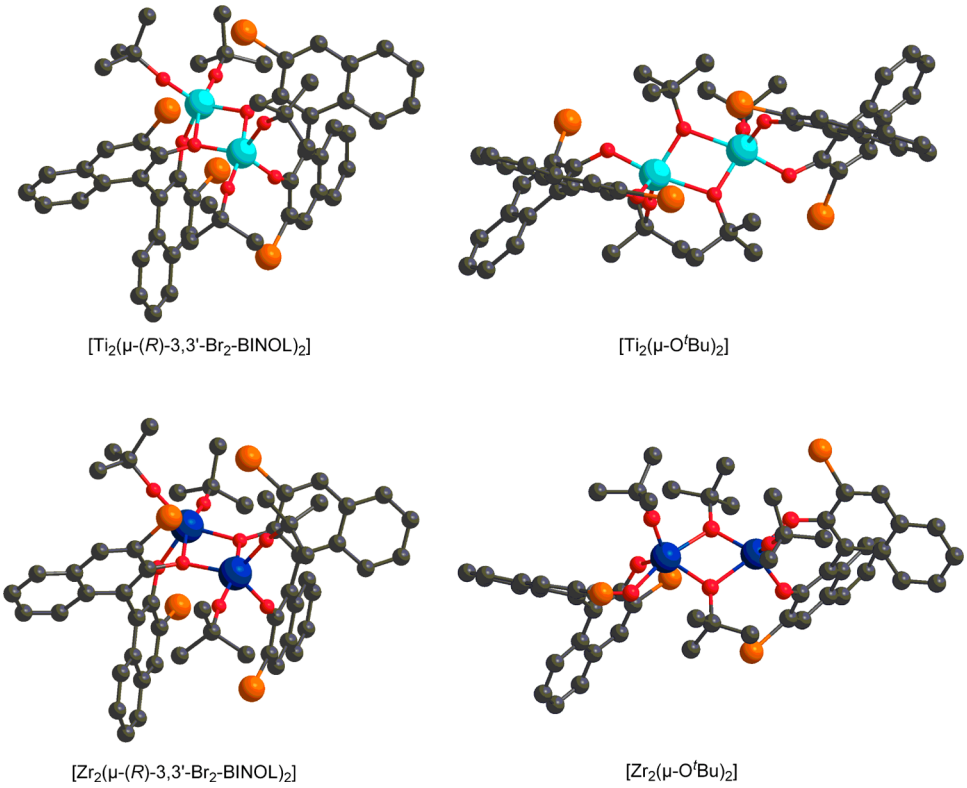

Figure 6. Optimized geometries for the dinuclear $[Ti_2\{(R)\text{-}3,3'\text{-}Br_2\text{–}BINOL\}_2(O^tBu)_4]$ and $[Zr_2\{(R)\text{-}3,3'\text{-}Br_2\text{–}BINOL\}_2(O^tBu)_4]$ complexes.

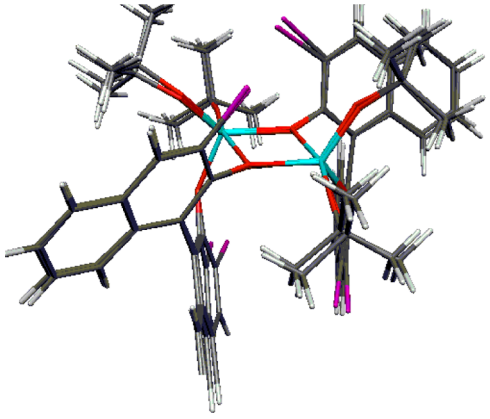

Figure 7. View of the experimental[21] and optimized molecular geometries for the titanium dinuclear complex.

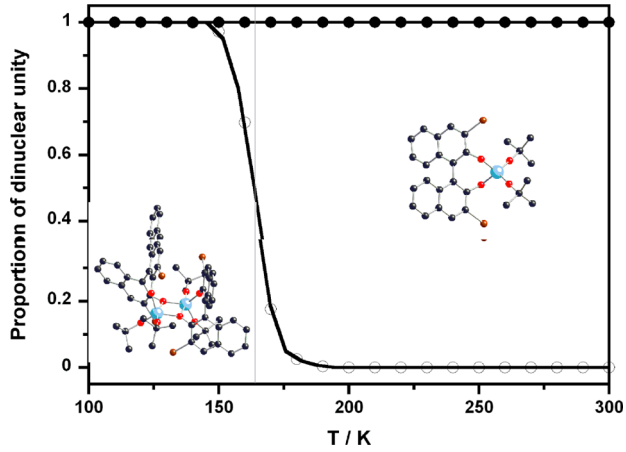

Figure 8. Proportion of the dinuclear complex for the titanium (open circles) and zirconium (black circles) systems as a function of the temperature.

the shorter metal–ligand bond distances (Ti–O = 1.979 and 2.270 Å vs Zr–O = 2.164 and 2.345 Å).

DFT electronic structure calculations have been also used to simulate the experimental ^{1}H NMR spectra (see Computational Details in Experimental Section). The chemical shifts (δ) corresponding to the hydrogen atoms from the 3,3′-Br_2–BINOL ligands in the mono- and dinuclear complexes of the titanium(IV) and zirconium(IV) systems are listed in Tables 2 and 3, respectively. The calculated δ values for the mononuclear titanium(IV) complex shows an almost complete equivalence of the corresponding H atoms from the two naphthyl units of each 3,3′-Br_2–BINOL ligand as experimentally observed at 303 K. On the other hand, the calculated δ values for the dinuclear titanium(IV) species evidence an unequivalence of the hydrogen atoms from the two naphthyl groups of each 3,3′-Br_2–BINOL ligand, as observed in the ^{1}H NMR spectrum at 203 K (Table 2). In both cases, the splitting of the proton signals of the $\{H_5\text{–}H_{5'}\}$, $\{H_6\text{–}H_{6'}\}$, and $\{H_7\text{–}H_{7'}\}$ pairs is smaller than that of the $\{H_4\text{–}H_{4'}\}$ and $\{H_8\text{–}H_{8'}\}$ pairs. This phenomenon is explained by the symmetry loss of the bridging binaphtol ligand in the dinuclear species when compared to the mononuclear one, providing thus additional evidence for the temperature-dependent dimerization reaction in the titanium-(IV) system.

Similarly, the calculated δ values for the dinuclear zirconium-(IV) species show the unequivalence of the hydrogen atoms from the two naphthyl groups of each 3,3′-Br_2–BINOL ligand in all the temperature range studied as experimentally observed in the ^{1}H NMR spectra at both 303 and 223 K (Table 3), which supports once again the only presence of the dinuclear

dx.doi.org/10.1021/jo3013594 | J. Org. Chem. 2012, 77, 10545–10556

Table 2. Calculated and Observed ^{1}H NMR Chemical Shifts (in ppm) in the Titanium(IV) System

atom	exp 303 K[a]	exp 203 K[a]	theo mono[b]	theo din[c]
H_4	8.11	8.24	8.10	8.16
$H_{4'}$		7.89	8.08	7.88
H_5	7.87	7.83	7.83	7.86
$H_{5'}$		7.92	7.83	7.89
H_6	7.36	7.35	7.52	7.53
$H_{6'}$		7.33	7.51	7.53
H_7	7.12	7.14	7.31	7.31
$H_{7'}$		7.05	7.30	7.26
H_8	7.00	7.00	7.17	7.28
$H_{8'}$		6.81	7.15	7.04

[a]Exp: experimental values. [b]Theo: theoretical values. Mono: mononuclear complex. [c]Din: dinuclear complex.

Table 3. Calculated and Observed ^{1}H NMR Chemical Shifts (in ppm) in the Zirconium(IV) System

atom	exp 303 K[a]	exp 223 K[a]	theo mono[b]	theo din[c]
H_4	8.25	8.26	8.11	8.12
$H_{4'}$	8.04	7.98	8.11	7.85
H_5	7.87	7.86	7.81	7.86
$H_{5'}$	7.91	7.92	7.81	7.88
H_6	7.42	7.40	7.49	7.55
$H_{6'}$	7.33	7.33	7.49	7.54
H_7	7.24	7.21	7.28	7.32
$H_{7'}$	7.08	7.07	7.28	7.26
H_8	7.19	7.10	7.05	7.23
$H_{8'}$	6.87	6.81	7.05	7.01

[a]Exp: experimental values. [b]Theo: theoretical values. Mono: mononuclear complex. [c]Din: dinuclear complex.

species in the zirconium(IV) system. Although the agreement between theoretical and experimental NMR spectra is only qualitative and, perhaps, it may be improved by including solvation effects, it is sufficiently adequate, and the trends of the simulated values match with the conclusions extracted from the experimental data and are in concordance with the stability of the species extrapolated previously from the DFT calculations.

Scope of the Enantioselective Friedel–Crafts Alkylation of Indoles with α,β-Unsaturated Ketones. The optimization of the reaction conditions for the Friedel–Crafts alkylation of indoles with enones has been reported in our previous communication.[18a] The optimized conditions involved the use of (*R*)-3,3′-Br_2–BINOL (20 mol %), $Zr(O^tBu)_4$ (20 mol %), indole **1** (0.15 mmol), and enone **2** (0.125 mmol) in CH_2Cl_2 (1.6 mL). Under these conditions, indole **1a** reacted with enone **2a** to give compound **3aa** with 87% yield and 97% ee. Under identical conditions, the $Hf(O^tBu)_4$-(*R*)-3,3′-Br_2–BINOL complex performed almost equal to the corresponding Zr complex. However, when $Ti(O^tBu)_4$ was used as a substitutive for $Zr(O^tBu)_4$, a sluggish reaction was observed providing compound **3aa** with low yield and almost racemic (6% ee) after 20 h.

The differences in catalytic activity and enantioselectivity between these complexes may be due in part to their different behavior in solution and the consequent different coordination geometries around the metal atom. Thus, the $Ti(O^tBu)_4$-(*R*)-3,3′-Br_2–BINOL, presumably a monomer, would lead to a slow nonenantioselective reaction, while the corresponding complexes of zirconium and hafnium, both with dimeric structure, would provide good yields and excellent enantioselectivities.[32] This result is also in agreement with the moderate positive nonlinear effect observed when correlating the enantiopurity of the Friedel–Crafts product **3aa** with the enantiopurity of ligand **L** (see Supporting Information, Figure S4), which suggests that the catalytic species should be a nonmonomeric Zr(IV)-(*R*)-3,3′-Br_2–BINOL complex (see also the Mechanistic Considerations section below). In fact, the ^{1}H NMR spectrum of the metal complex generated from racemic 3,3′-Br_2–BINOL and $Zr(O^tBu)_4$ showed two singlets at δ 8.04 and 8.25 ppm corresponding to protons H_4 and $H_{4'}$ in the homodimer, together with two singlets at δ 8.12 and 8.29 corresponding to these protons in the heterodimer complex. The relative integration of these signals indicates a ca. 2:1 ratio of heterodimer vs homodimer complexes.[33]

The $[Zr_2\{(R)\text{-}3,3'\text{-}Br_2\text{–}BINOL\}_2(O^tBu)_4]$ catalyst can be successfully applied to the Friedel–Crafts alkylation of indole **1a** and a number of α,β-unsaturated ketones **2b–2l**, bearing an aromatic ring bound to the carbonyl group and an aliphatic chain linked to the C–C double bond, to give the corresponding chiral alkylated indoles **3ab–3al** with good yields and ee above 95% in most of the cases (Table 4). We

Table 4. Enantioselective Friedel–Crafts Reaction of Indole (1a) with Enones 2a–2l Catalyzed by $Zr(O^tBu)_4$-L.[a]

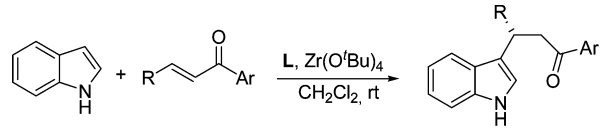

1a **2** **3**

entry	2	Ar	R	time (h)	3	yield (%)[b]	ee (%)[c]
1	**2a**	Ph	Me	3	**3aa**	87	97
2	**2b**	Ph	Et	20	**3ab**	87	94
3	**2c**	Ph	Pr	24	**3ac**	82	97
4	**2d**	Ph	Ph	96	**3ad**	25	96
5	**2e**	*p*-Me-C_6H_4	Me	20	**3ae**	91	95
6	**2f**	*m*-MeC_6H_4	Me	4	**3af**	84	92
7	**2g**	*o*-Me-C_6H_4	Me	22	**3ag**	73	72
8	**2h**	*p*-MeOC_6H_4	Me	18	**3ah**	54	95
9	**2i**	*p*-F-C_6H_4	Me	2	**3ai**	92	96
10	**2j**	*p*-Br-C_6H_4	Me	2	**3aj**	95	97
11	**2k**	2-naphthyl	Me	2	**3ak**	89	98
12	**2l**	2-thienyl	Me	20	**3al**	87	96

[a]Reaction carried out with **1a** (0.15 mmol, 1.2 equiv), **2** (0.125 mmol, 1 equiv), (*R*)-**L** (0.025 mmol, 20 mol %), $Zr(O^tBu)_4$ (0.025 mmol, 20 mol %) in CH_2Cl_2 (1.6 mL) under N_2 atmosphere at rt. [b]Isolated yield of **3**. [c]Determined by HPLC analysis on chiral stationary phases.

report here also the reaction with differently substituted indoles **1b–1j** with α,β-unsaturated ketone **2a** (Table 5). Indole derivatives with either electron-donating (CH_3, CH_3O) or electron-withdrawing substituents (F, Cl) at 5- or 6-positions were competent substrates affording the alkylated products with excellent enantioselectivity (entries 5–6 and 8). However substitution at 1-, 2- or 7-positions (entries 1–2 and 9) brings about a notable drop in reactivity and, besides in the case of substituents at 1- or 7-positions, a drastic drop of enantioselectivity (6 and 20% ee, respectively, entries 1 and 9). Although these last results are disappointing from the synthetic point of view, they are very interesting to make a

dx.doi.org/10.1021/jo3013594 | J. Org. Chem. 2012, 77, 10545–10556

Table 5. Enantioselective Friedel–Crafts Reaction of Indole Derivatives 1b–1j with α,β-Unsaturated Ketone 2a Catalyzed by $Zr(O^tBu)_4$-L[a]

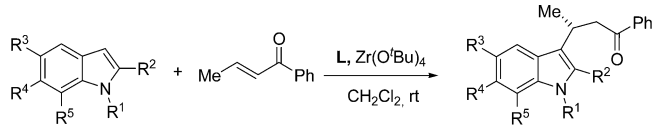

entry	1	R_1	R_2	R_3	R_4	R_5	time (h)	3	yield (%)[b]	ee (%)[c]
1	**1b**	Me	H	H	H	H	36	**3ba**	75	6
2	**1c**	H	Me	H	H	H	36	**3ca**	64	70
3	**1d**	H	H	Me	H	H	4	**3da**	97	95
4	**1e**	H	H	MeO	H	H	4	**3ea**	95	97
5	**1f**	H	H	F	H	H	4	**3fa**	94	97
6	**1g**	H	H	Cl	H	H	30	**3ga**	74	95
7	**1h**	H	H	H	Me	H	8	**3ha**	72	94
8	**1i**	H	H	H	F	H	19	**3ia**	96	94
9	**1j**	H	H	H	H	Me	40	**3ja**	57	20

[a]Reaction carried out with **1** (0.15 mmol, 1.2 equiv), **2a** (0.125 mmol, 1 equiv), (*R*)-**L** (0.025 mmol, 20 mol %), $Zr(O^tBu)_4$ (0.025 mmol, 20 mol %) in CH_2Cl_2 (1.6 mL) under N_2 atmosphere at rt. [b]Isolated yield of **3**. [c]Determined by HPLC analysis on chiral stationary phases.

mechanistic proposal for the Friedel–Crafts alkylation (see later).

Mechanistic Considerations on the Friedel–Crafts Alkylation of Indoles with α,β-Unsaturated Ketones Catalyzed by $[Zr_2\{(R)\text{-}3,3'\text{-}Br_2\text{–}BINOL\}_2(O^tBu)_4]$. Once the structure of the catalytic species was established, we carried out spectroscopic studies of this species in the presence of the starting materials, the α,β-unsaturated ketone **2a** and indole **1a**. Binding of the enone to the zirconium center was examined for the $[Zr_2\{(R)\text{-}3,3'\text{-}Br_2\text{–}BINOL\}_2(O^tBu)_4]$ catalyst by NMR spectroscopy studies. Apparently, the coordination of the enone to the catalyst does not cause significant structural change in the complex structure; only the singlet signal due to protons H4′ (δ 8.04 ppm) in *ortho* to the bromine atoms of the ligand experiences a broadening of the signal, and the rest of ^1H resonances, corresponding to the complex, remain almost unaltered. The broadening of this signal seems to indicate that after the coordination of the enone, both protons H4′ are not fully equivalent, which suggests that only one of the zirconium atoms is coordinated to the enone and most probably the reaction should occur on a single zirconium center of the catalyst. On the other hand, coordination of the enone to the zirconium ion produced a downfield shift of the signal corresponding to the enone β carbon from 144.93 to 145.20 ppm in the ^{13}C NMR spectra. To further ascertain the maintenance of the dimeric zirconium complex after coordination of the enone, we repeated these experiments with a substrate analogue such as *N*,*N*-dimethylformamide (DMF).[34] After addition of 1 equiv of DMF to the complex formed from equimolar amounts of (*R*)-3,3′-Br_2–BINOL and $Zr(O^tBu)_4$, a clear upfield shift of the signals corresponding to the CH (from 7.95 to 6.25 ppm) and methyl groups (from 2.90 and 2.81 to 2.01 and 1.62 ppm) of the DMF was observed, indicating the strong coordination of the DMF molecule to the zirconium atoms. More importantly, the set of signals corresponding to the zirconium complex was maintained, although all the signals experienced an upfield shift, indicating that coordination of DMF does not break up the dimer complex (see Supporting Information).

Once we observed that the addition of the enone to the catalyst did not break the dimeric zirconium complex, we continued the spectroscopic study by adding indole to the catalyst–enone mixture, which gave rise to an uninterpretable ^1H NMR spectrum. However, on the basis of the low enantioselectivity observed in the alkylation of *N*-methyl indole (**1b**), we assume that the presence of the N–H indole is necessary to establish a hydrogen bond with one of the basic oxygen atoms of the (*R*)-3,3′-Br_2–BINOL. It suggests a bifunctional mode of action of catalyst $Zr(O^tBu)_4$-(*R*)-**L**, with simultaneous activation of the α,β-unsaturated ketone by the Zr atom, and of the indole through coordination of the N–H with a (*R*)-3,3′-Br_2–BINOLate oxygen.[35] The lower levels of stereoinduction observed in the cases of 2- and especially 7-substituted indoles seem to corroborate the preceding hypothesis since the nearness of the substituents to N–H of indole will make difficult the aforementioned coordination.

The (*R*)-configuration for the stereogenic center was assigned by comparison of the optical rotation signs of **3aa** and **3ea** with literature data[36] and by X-ray crystallographic analysis of **3ga** (see Supporting Information).[37] For the rest of products **3** it was assigned on the assumption of a uniform mechanistic pathway: To explain the stereochemical outcome of the reaction, we propose the stereomodel shown in Figure 9, in which the *Si* face of the double bond is blocked by a nearby naphthyl subunit, leaving the *Re* face of the enone more accessible to be attacked by the indole. Figure 9 shows also that

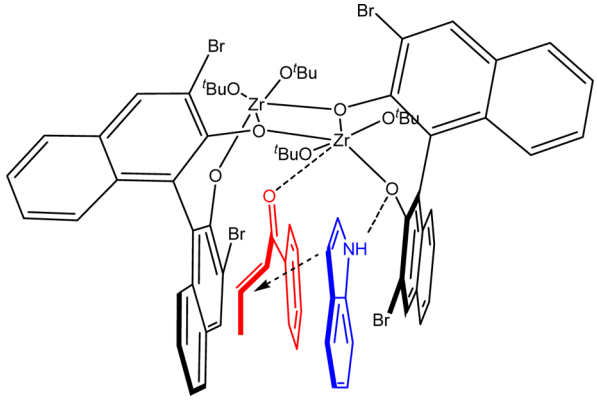

Figure 9. Proposed stereomodel for the bifunctional mode of action of the catalyst.

dx.doi.org/10.1021/jo3013594 | J. Org. Chem. 2012, 77, 10545–10556

the H atom of the N−H of the indole must form a hydrogen bond with the oxygen atom of the binaphthol ligand, which would play an important role in stabilizing the transition state of the process. Accordingly, the absence of the hydrogen bond interaction in the case of *N*-methylindole (**1b**) might explain why a lower ee was obtained (75% yield, 6% ee) in the reaction with enone **2a**. A bifunctional mode of action of catalyst $[Zr_2\{(R)\text{-}3,3'\text{-}Br_2\text{−}BINOL\}_2(O^tBu)_4]$ (**A**) is therefore proposed with simultaneous activation of the enone by the metal center and of the indole by the oxygen atoms of the ligand through coordination with the N−H. A plausible mechanism (Scheme 2) for the $Zr(O^tBu)_4$-(*R*)-**L** catalyzed Friedel−Crafts

Scheme 2. Proposed Catalytic Cycle for the Friedel−Crafts Alkylation of Indole with *α,β*-Unsaturated Ketones Catalyzed by $[Zr_2\{(R)\text{-}3,3'\text{-}Br_2\text{−}BINOL\}_2(O^tBu)_4]$

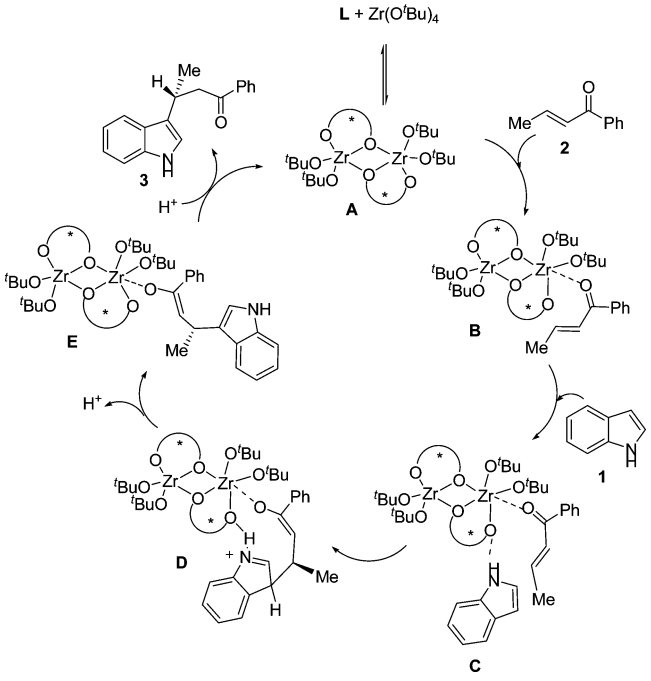

reaction between indoles and enones involves activation of the enone by coordination with a Zr(IV) atom of the catalyst **A** to form a substrate-catalyst complex **B**,[38] which undergoes H-bond assisted (**C**) nucleophilic addition of the indole to the *Re* face of the double bond of the enone to provide the Friedel−Crafts adduct **D**. Subsequently, H-transfer and decoordination of the chiral enolate **E** affords the Friedel−Crafts product and regenerates the catalyst **A**.

CONCLUSIONS

In summary, an experimental and theoretical study on the structure of complexes based in (*R*)-3,3′-Br_2−BINOL and group (IV) metals used as catalyst in an enantioselective Friedel−Crafts alkylation of indoles with *α,β*-unsaturated ketones has been carried out. NMR spectroscopic studies of these complexes have been performed, which suggested that at room temperature the catalyst would have a monomeric structure in the case of Ti(IV) and a dimeric structure in the case of Zr(IV) and Hf(IV). NLE studies revealed that the zirconium species involved in the catalysis should contain more than one (*R*)-3,3′-Br_2−BINOL unit. Density functional theory (DFT) calculations clearly corroborate these experimental studies. The dimeric structure with a doubly bridged motif $[Zr^{IV}_2\{\mu\text{-}(R)\text{-}Br_2\text{−}BINOL\}_2]$ where each binaphthol ligand acts as bridge between the metal centers (Novak's model) is more stable than the dimeric structure with a doubly bridged motif $[Zr^{IV}_2(\mu\text{-}O^tBu)_2]$ where the *tert*-butoxide groups act as bridging ligands (Kobayashi's model). A plausible mechanism for the Friedel−Crafts alkylation of indoles with *α,β*-unsaturated ketones and a stereomodel for the bifunctional mode of action of the catalyst that explains the observed stereochemistry in the reaction products have been proposed.

EXPERIMENTAL SECTION[39]

Preparation and Characterization of the Chiral Metal Complexes. *[Ti{(R)-3,3′-Br_2−BINOL}(O^tBu)$_2$]*. $Ti(O^tBu)_4$ (8 μL, 0.025 mmol) was added via syringe to a solution of ligand **L** (11.1 mg, 0.025 mmol) in CD_2Cl_2 (0.5 mL) under nitrogen atmosphere at rt: ^{1}H NMR (400 MHz, CD_2Cl_2) *δ* 8.11 (s, 2H, H-4), 7.87 (dd, *J* = 8.1, 0.5 Hz, 1H, H-5), 7.36 (ddd, *J* = 8.0, 6.7, 1.1 Hz, 2H, H-6), 7.12 (ddd, *J* = 8.2, 6.7, 1.3 Hz, 2H, H-7), 7.00 (d, *J* = 8.4 Hz, 2H, H-8), 1.06 (s, 18H, 2 ^{t}Bu); ^{13}C NMR (100.1 MHz, CD_2Cl_2) *δ* 158.0 (C), 132.9 (C), 132.0 (CH), 130.6 (C),127.7 (CH), 127.2 (CH), 125.3 (CH), 124.0 (CH), 120.0 (C), 117.9 (C), 80.0 (C), 31.3 (CH_3).

[Zr_2{(R)-3,3′-Br_2−BINOL}$_2$(O^tBu)$_4$]. $Zr(O^tBu)_4$ (10 μL, 0.025 mmol) was added via syringe to a solution of ligand **L** (11.1 mg, 0.025 mmol) in CD_2Cl_2 (0.5 mL) under nitrogen atmosphere at rt: ^{1}H NMR (400 MHz, CD_2Cl_2) *δ* 8.25 (s, 1H, H-4), 8.04 (s, 1H, H-4′), 7.90 (d, *J* = 8.1 Hz, 1H, H-5′), 7.87 (d, *J* = 8.1 Hz, 1H, H-5), 7.41 (ddd, *J* = 8.1, 6.7, 1.2 Hz, 1H, H-6), 7.33 (ddd, *J* = 8.0, 6.8, 1.1 Hz, 1H, H-6′), 7.24 (ddd, *J* = 8.6, 6.7, 1.3 Hz, 1H, H-7), 7.18 (d, *J* = 8.1 Hz, 1H, H-8), 7.08 (ddd, *J* = 8.3, 6.8, 1.3 Hz, 1H, H-7′), 6.86 (d, *J* = 8.5 Hz, 1H, H-8′), 0.96 (s, 9H, ^{t}Bu), 0.95 (s, 9H, ^{t}Bu); ^{13}C NMR (100.1 MHz, CD_2Cl_2) *δ* 154.3 (C), 152.7 (C), 133.6 (C), 132.6 (C), 132.5 (CH), 130.64 (CH), 130.57 (C), 130.1 (C), 127.6 (CH), 127.3 (CH), 127.1 (CH), 127.0 (CH), 126.4 (CH), 125.3 (CH), 124.9 (CH), 123.4 (CH), 122.0 (C), 119.3 (C), 117.5 (C), 117.0 (C), 79.4 (C), 78.9 (C), 32.1 (CH_3), 31.6 (CH_3).

[Hf_2{(R)-3,3′-Br_2−BINOL}$_2$(O^tBu)$_4$]. $Hf(O^tBu)_4$ (11 μL, 0.025 mmol) was added via syringe to a solution of ligand **L** (11.1 mg, 0.025 mmol) in CD_2Cl_2 (0.5 mL) under nitrogen atmosphere at rt: ^{1}H NMR (400 MHz, CD_2Cl_2) *δ* 8.27 (s, 1H, H-4), 8.06 (s, 1H, H-4′), 7.91 (dd, *J* = 8.1, 0.5 Hz, 1H, H-5′), 7.88 (d, *J* = 8.2 Hz, 1H, H-5), 7.42 (ddd, *J* = 8.1, 6.7, 1.3 Hz, 1H, H-6), 7.33 (ddd, *J* = 8.0, 6.8, 1.1 Hz, 1H, H-6′), 7.25 (ddd, *J* = 8.1, 6.7, 1.3 Hz, 1H, H-7), 7.18 (d, *J* = 8.1 Hz, 1H, H-8), 7.08 (ddd, *J* = 8.3, 6.8, 1.3 Hz, 1H, H-7′), 6.86 (dd, *J* = 8.5, 0.4 Hz, 1H, H-8′), 0.95 (s, 9H, ^{t}Bu), 0.94 (s, 9H, ^{t}Bu); ^{13}C NMR (100.1 MHz, CD_2Cl_2) *δ* 154.0 (C), 151.9 (C), 132.5 (C), 132.6 (CH), 132.5 (C), 130.8 (C), 130.7 (CH), 130.1 (C),127.5 (CH), 127.4 (CH), 127.1 (CH), 126.8 (CH), 126.4 (CH), 125.3 (CH), 125.1 (CH), 123.5 (CH), 122.6 (C), 119.3 (C), 117.5 (C), 117.2 (C), 78.4 (C), 78.0 (C), 32.3 (CH_3), 31.8 (CH_3).

Computational Details. Electronic structure calculations based on the density functional theory (DFT) using the hybrid B3LYP functional and the quadratic convergence approach were performed through the Gaussian09 package.[25] Double-*ζ* all electron basis set proposed by Ahlrichs et al. was used for the hydrogen, carbon and oxygen atoms.[26] Dunning's LANL2DZ basis set[27] and their pseudopotential functions[28] were used for the valence and the internal electrons of the titanium, zirconium and bromide atoms. Molecular geometries for all species considered in this study were optimized. The stable species were determined from the energy in the minimal point of the potential curve, from the zero-point energy, i.e., from the energy in the zero vibrational level and from the free energy at several temperatures. In the last cases, and considering a gas phase, the electronic, vibrational, translational and rotational contributions to the free energy (enthalpy and entropy) were taken into account. NMR shielding tensors were computed with the continuous set of gauge transformations (CSGT)[29] method and the gauge-independent atomic orbital (GIAO)[30] method. Independently, the ^{1}H NMR spectrum of

dx.doi.org/10.1021/jo3013594 | J. Org. Chem. 2012, 77, 10545−10556

tetramethylsilane (TMS) was calculated to be used as reference. Similar results were obtained for the NMR chemical shifts using different basis sets to build the atomic orbitals, even when basis sets optimized for these kinds of calculations were used.

Typical Procedure for the Asymmetric Friedel–Crafts Alkylation. To a solution of ligand **L** (11.1 mg, 0.025 mmol) in dry CH_2Cl_2 (0.8 mL) at rt under argon was added $Zr(O^tBu)_4$ (10 μL, 0.025 mmol). The mixture was stirred for 1 h, and then a solution of indole **1** (0.15 mmol) and enone **2** (0.125 mmol) in dry CH_2Cl_2 (0.8 mL) was added via syringe. The reaction mixture was monitorized by TLC until starting material was completely reacted. Water (10 mL) was added, and the mixture was extracted with EtOAc (3 × 20 mL), washed with brine (10 mL) and dried ($MgSO_4$). Product **3** was obtained pure after column chromatography. For characterization data for compounds **3aa**–**3al**, see ref 18a.

*(R)-(+)-3-(1-Methyl-1H-indol-3-yl)-1-phenylbutan-1-one (**3ba**).* From enone **2a** (18.8 mg, 0.125 mmol), 25.9 mg (75%) of compound **3ba** were obtained. Enantiomeric excess was determined by HPLC (Chiralcel OD-H, 10% isopropanol-90% hexane, 1.0 mL/min): $(R)_{major}$ t_R = 10.3 min, $(S)_{minor}$ t_R = 11.9 min, to be 6%; yellow oil; $[\alpha]_D^{25}$ + 14.9 (*c* 0.76, $CHCl_3$); MS (EI) *m*/*z* (%) 277 (M^+, 28), 159 (15), 158 (100), 105 (17), 77 (13); HRMS 277.1467 (M^+), $C_{19}H_{19}NO$ required 277.1467; ^1H NMR (300 MHz, $CDCl_3$) δ 7.95 (d, *J* = 7.8 Hz, 2H), 7.66 (d, *J* = 7.8 Hz, 1H), 7.53 (t, *J* = 7.5 Hz, 1H), 7.43 (t, *J* = 7.8 Hz, 2H), 7.28 (d, *J* = 8.1 Hz, 1H), 7.22 (td, *J* = 7.2, 1.2 Hz, 1H), 7.10 (td, *J* = 7.5, 1.2 Hz, 1H), 6.9 (s, 1H), 3.82 (m, 1H), 3.73 (s, 3H), 3.46 (dd, *J* = 16.1, 5.0 Hz, 1H), 3.22 (dd, *J* = 16.3, 8.9 Hz, 1H), 1.44 (d, *J* = 6.6 Hz, 3H); ^{13}C NMR (75.5 MHz, $CDCl_3$) δ 199.8 (C), 137.4 (C), 137.3 (C), 133.0 (CH), 128.7 (CH), 128.2 (CH), 126.8 (C), 125.2 (CH), 121.7 (CH), 120.2 (C), 119.4 (CH), 118.8 (CH), 109.5 (CH), 46.8 (CH_2), 32.7 (CH_3), 27.2 (CH), 21.3 (CH_3).

*(R)-(−)-3-(2-Methyl-1H-indol-3-yl)-1-phenylbutan-1-one (**3ca**).* From enone **2a** (18.8 mg, 0.125 mmol), 22.2 mg (64%) of compound **3ca** were obtained. Enantiomeric excess was determined by HPLC (Chiralcel OD-H, 15% isopropanol-85% hexane, 0.5 mL/min): $(R)_{major}$ t_R = 22.9 min, $(S)_{minor}$ t_R = 28.1 min; to be 70%; yellow oil; $[\alpha]_D^{25}$ −37.3 (*c* 0.52, $CHCl_3$); MS (EI) *m*/*z* (%) 277 (M^+, 21), 173 (17), 162 (18), 158 (100), 146 (18), 105(42), 77 (40); HRMS 277.1441 (M^+), $C_{19}H_{19}NO$ required 277.1467; ^1H NMR (300 MHz, $CDCl_3$) δ 7.87 (d, *J* = 7.5 Hz, 2H), 7.70–7.65 (m, 2H), 7.49 (t, *J* = 7.2 Hz, 1H), 7.37 (t, *J* = 7.5 Hz, 2H), 7.25–7.21 (m, 1H), 7.11–7.04 (m, 2H), 3.75 (m, 1H), 3.54 (dd, *J* = 16.2, 6.3 Hz, 1H), 3.38 (dd, *J* = 16.2, 7.5 Hz, 1H), 2.37 (s, 1H), 1.51 (d, *J* = 7.2 Hz, 3H); ^{13}C NMR (75.5 MHz, $CDCl_3$) δ 200.2 (C), 137.4 (C), 135.6 (C), 132.9 (CH), 130.5 (C), 128.6 (CH), 128.2 (CH), 127.2 (C), 120.8 (CH), 119.1 (CH), 119.0 (CH), 115.6 (C), 110.7 (C), 45.8 (CH_2), 27.5 (CH), 21.2 (CH_3), 12.1 (CH_3).

*(R)-(+)-3-(5-Methyl-1H-indol-3-yl)-1-phenylbutan-1-one (**3da**).* From enone **2a** (18.8 mg, 0.125 mmol), 33.6 mg (97%) of compound **3ca** were obtained. Enantiomeric excess was determined by HPLC (Chiracel OD-H), hexane:*i*-PrOH 80:20, 1 mL/min: $(S)_{minor}$ t_r = 8.8 min, $(R)_{major}$ t_r = 15.7 min, to be 95%; crystalline solid, mp 99–102 °C (CH_2Cl_2-hexane); $[\alpha]^{25}{}_D$= +44.8 (*c* 1.2, $CHCl_3$); MS(EI) 277 (M^+, 36), 172 (22), 158 (100), 105 (16); HRMS 277.1462, $C_{19}H_{19}NO$ required 277.1467; ^1H NMR ($CDCl_3$) δ 7.97 (dd, *J* = 7.2, 1.5 Hz, 2H), 7.88 (br s, 1H), 7.56 (tt, *J* = 7.4, 1.5 Hz, 1H), 7.48–7.43 (m, 3H), 7.25 (d, *J* = 8.4 Hz, 1H), 7.03 (dd, *J* = 8.4, 0.9 Hz, 1H), 6.99 (d, *J* = 2.4 Hz, 1H), 3.82 (m, 1H), 3.47 (dd, *J* = 16.4, 4.7 Hz, 1H), 3.24 (dd, *J* = 16.4, 9.2 Hz, 1H), 2.47 (s, 3H), 1.45 (d, *J* = 6.9 Hz, 3H); ^{13}C NMR ($CDCl_3$) δ 200.0 (C), 137.5 (C), 134.9 (C), 133.1 (CH), 128.7 (CH), 128.6 (C), 128.3 (CH), 126.7 (C), 123.68 (CH), 121.2 (C), 120.5 (CH), 119.0 (CH), 111.1 (CH), 46.9 (CH_2), 27.3 (CH), 21.6 (CH_3), 21.1 (CH_3).

*(R)-(+)-3-(5-Methoxy-1H-indol-3-yl)-1-phenylbutan-1-one (**3ea**).* From enone **2a** (18.8 mg, 0.125 mmol), 34.8 mg (95%) of compound **3ea** were obtained. Enantiomeric excess was determined by HPLC (Chiracel OD-H), hexane:*i*-PrOH 80:20, 0.5 mL/min: $(S)_{minor}$ t_R = 20.4 min, $(R)_{major}$ t_R = 22.1 min, to be 97%; yellow oil; $[\alpha]^{25}{}_D$= +52.1 (*c* 1.4, $CHCl_3$); ^1H and ^{13}C NMR data were coincident with those reported in the literature.[34]

*(R)-(+)-3-(5-Fluoro-1H-indol-3-yl)-1-phenylbutan-1-one (**3fa**).* From enone **2a** (18.8 mg, 0.125 mmol), 33.0 mg (94%) of compound **3fa** were obtained. Enantiomeric excess was determined by HPLC (Chiralcel OD-H, hexane:*i*-PrOH 90:10, 1.0 mL/min): $(S)_{minor}$ t_R = 16.4 min, $(R)_{major}$ t_R = 25.6 min, to be 97%; yellow oil; $[\alpha]_D^{25}$ + 20.0 (*c* 1.6, $CHCl_3$); MS (EI) *m*/*z* (%) 281 (M^+, 27), 176 (22), 162 (100), 105(32), 77 (20); HRMS 281.1218 (M^+), $C_{18}H_{16}FNO$ required 281.1216; ^1H NMR (300 MHz, $CDCl_3$) δ 8.08 (br s, 1H), 7.95 (dd, *J* = 8.0, 1.5 Hz, 2H), 7.56 (tt, *J* = 7.4, 1.5 Hz, 1H), 7.45 (t, *J* = 7.5 Hz, 2H), 7.31 (dd, *J* = 9.9, 2.4 Hz, 1H), 7.25 (dd, *J* = 9.0, 4.2 Hz, 1H), 7.05 (d, *J* = 2.4 Hz, 1H), 6.93 (d, *J* = 9.0, 2.6 Hz, 1H), 3.83–3.72 (m, 1H), 3.44 (dd, *J* = 16.5, 5.4 Hz, 1H), 3.24 (dd, *J* = 16.4, 8.6 Hz, 1H), 1.44 (d, *J* = 6.9 Hz, 3H); ^{13}C NMR (75.5 MHz, $CDCl_3$) δ 199.8 (C), 157.7 (d, J_{C-F} = 232.8 Hz, C), 137.3 (C), 133.2 (CH), 133.1 (C), 128.7 (CH), 128.2 (CH), 126.8 (d, J_{C-F} = 9.5 Hz, C), 122.2 (CH), 121.7 (d, J_{C-F} = 4.7 Hz, C), 111.8 (d, *J* = 9.7 Hz, CH), 110.5 (d, J_{C-F} = 26.2 Hz, CH), 104.3 (d, J_{C-F} = 23.3 Hz, CH), 46.3 (CH_2), 27.2 (CH), 21.1 (CH_3).

*(R)-(+)-3-(5-Chloro-1H-indol-3-yl)-1-phenylbutan-1-one (**3ga**).* From enone **2a** (18.8 mg, 0.125 mmol), 27.5 mg (74%) of compound **3ga** were obtained. Enantiomeric excess was determined by HPLC (Chiracel OD-H), hexane:*i*-PrOH 90:10, 1 mL/min: $(S)_{minor}$ t_r = 16.1 min, $(R)_{major}$ t_r = 24.4 min, to be 95%; crystalline solid, mp 134–137 °C (CH_2Cl_2-hexane); $[\alpha]^{25}{}_D$= +38.6 (*c* 0.7, $CHCl_3$); MS(EI) 297 (M^+, 17), 192 (22), 180 (31), 178 (100), 143 (30), 105(47), 77 (41); HRMS 297.0913, $C_{18}H_{16}ClNO$ required 297.0920; ^1H NMR ($CDCl_3$) δ 8.17 (br s, 1H), 7.95 (dd, *J* = 7.5, 1.5 Hz, 2H), 7.63 (d, *J* = 1.8 Hz, 1H), 7.56 (tt, *J* = 7.5, 2.1 Hz, 1H), 7.45 (t, *J* = 7.5 Hz, 2H), 7.23 (d, *J* = 9.3 Hz, 1H), 7.13 (dd, *J* = 8.7, 1.8 Hz, 1H), 7.01 (d, *J* = 2.4 Hz, 1H), 3.78 (m, 1H), 3.43 (dd, *J* = 16.4, 5.3 Hz, 1H), 3.25 (dd, *J* = 16.4, 8.4 Hz, 1H), 1.44 (d, *J* = 6.9 Hz, 3H); ^{13}C NMR ($CDCl_3$) δ 199.8 (C), 137.2 (C), 135.0 (C), 133.2 (CH), 128.7 (CH), 128.2 (CH), 127.5 (C), 125.0 (C), 122.4 (CH), 121.9 (CH), 121.2 (C), 118.8 (CH), 112.4 (CH), 46.4 (CH_2), 27.2 (CH), 21.3 (CH_3).

*(R)-(+)-3-(6-Methyl-1H-indol-3-yl)-1-phenylbutan-1-one (**3ha**).* From enone **2a** (18.8 mg, 0.125 mmol), 24.9 mg (72%) of compound **3ha** were obtained. Enantiomeric excess was determined by HPLC (Chiralpack AD-H, hexane:*i*-PrOH 90:10, 1.0 mL/min): $(S)_{minor}$ t_R = 23.8 min, $(R)_{major}$ t_R = 28.5 min, to be 94%; crystalline solid, mp 105–108 °C (CH_2Cl_2-hexane); $[\alpha]_D^{25}$ + 25.1 (*c* 1.5, $CHCl_3$); MS (EI) *m*/*z* (%) 277 (M^+, 29), 172 (30), 158 (100), 105 (52), 77 (21); HRMS 277.1473 (M^+), $C_{19}H_{19}NO$ required 277.1467; ^1H NMR (300 MHz, $CDCl_3$) δ 7.95 (dd, *J* = 8.1, 1.8 Hz, 2H), 7.82 (br s, 1H), 7.57–7.52 (m, 2H), 7.44 (t, *J* = 7.5 Hz, 2H), 7.16 (s, 1H), 6.97–6.95 (m, 2H), 3.87–3.74 (m, 1H), 3.47 (dd, *J* = 16.2, 4.8 Hz, 1H), 3.23 (dd, *J* = 16.2, 9.0 Hz, 1H), 2.46 (s, 3H), 1.44 (d, *J* = 6.9 Hz, 3H); ^{13}C NMR (75.5 MHz, $CDCl_3$) δ 199.9 (C), 137.4 (C), 137.2 (C), 133.1 (CH), 132.0 (C), 128.7 (CH), 128.3 (CH), 124.3 (C), 121.6 (C), 121.2 (CH), 119.6 (CH), 119.0 (CH), 111.4 (CH), 46.6 (CH_2), 27.3 (CH), 21.8 (CH_3), 21.1 (CH_3).

*(R)-(+)-3-(6-Fluoro-1H-indol-3-yl)-1-phenylbutan-1-one (**3ia**).* From enone **2a** (18.8 mg, 0.125 mmol), 33.7 mg (96%) of compound **3ia** were obtained. Enantiomeric excess was determined by HPLC (Chiralpack AD-H, hexane:*i*-PrOH 90:10, 1.0 mL/min): $(S)_{minor}$ t_R = 20.6 min, $(R)_{major}$ t_R = 23.4 min, to be = 94%; yellow oil; $[\alpha]_D^{25}$ + 24.6 (*c* 1.15, $CHCl_3$; MS (EI) *m*/*z* (%) 281 (M^+, 52), 176 (43), 162 (100), 105(20), 77 (19); HRMS 281.1216 (M^+), $C_{18}H_{16}FNO$ required 281.1216; ^1H NMR (300 MHz, $CDCl_3$) δ 8.04 (br s, 1H), 7.95 (dd, *J* = 8.0, 1.5 Hz, 2H), 7.59–7.53 (m, 2H), 7.45 (t, *J* = 7.4 Hz, 2H), 7.02 (dd, *J* = 9.6, 2.1 Hz, 1H), 6.98 (d, *J* = 1.8 Hz, 1H), 6.89 (ddd, *J* = 9.6, 9.0, 2.3 Hz, 1H), 3.87–3.75 (m, 1H), 3.44 (dd, *J* = 16.5, 5.1 Hz, 1H), 3.24 (dd, *J* = 16.4, 8.6 Hz, 1H), 1.44 (d, *J* = 6.9 Hz, 3H); ^{13}C NMR (75.5 MHz, $CDCl_3$) δ 199.9 (C), 160.1 (d, J_{C-F} = 236.1 Hz, C), 137.4 (C), 136.6 (d, J_{C-F} = 12.4 Hz, C), 133.2 (C), 128.7 (CH), 128.2 (CH), 123.1 (C), 121.7 (C), 120.5 (d, J_{C-F} = 3.5 Hz, CH), 120.0 (d, J_{C-F} = 10.0 Hz, CH), 108.1 (d, J_{C-F} = 24.2 Hz, CH), 97.7 (d, J_{C-F} = 25.7 Hz, CH), 46.5 (CH_2), 27.2 (CH), 21.2 (CH_3).

*(R)-3-(+)-7-Methyl-1H-indol-3-yl)-1-phenylbutan-1-one (**3ja**).* From enone **2a** (18.8 mg, 0.125 mmol), 19.8 mg (57%) of compound **3ja** were obtained. Enantiomeric excess was determined by HPLC

dx.doi.org/10.1021/jo3013594 | J. Org. Chem. 2012, 77, 10545–10556

(Chiralpack AD-H, hexane:*i*-PrOH 90:10, 1.0 mL/min): $(S)_{minor}$ t_R = 13.2 min, $(R)_{major}$ t_R = 15.1 min, to be = 20%; crystalline solid; mp 118−121 °C (CH_2Cl_2-hexane); $[\alpha]_D^{25}$ + 5.8 (*c* 0.48, $CHCl_3$); MS (EI) *m*/*z* (%) 277 (M^+, 27), 159 (13), 158 (100), 143 (11), 105 (20), 77 (21); HRMS 277.1468 (M^+), $C_{19}H_{19}NO$ required 277.1467; ^1H NMR (300 MHz, $CDCl_3$) δ 7.95 (d, *J* = 7.5 Hz, 2H), 7.90 (s, 1H), 7.57−7−52 (m, 2H), 7.44 (t, *J* = 7.65 Hz, 2H), 7.08−6.99 (m, 3H), 3.83 (m, 1H), 3.48 (dd, *J* = 16.8, 4.8 Hz, 1H), 3.24 (dd, *J* = 16.7, 8.9 Hz, 1H), 2.48 (s, 3H), 1.45 (d, *J* = 7.2 Hz, 3H); ^{13}C NMR (75.5 MHz, $CDCl_3$) δ 199.9 (C), 137.4 (C), 136.3 (C), 133.1 (CH), 128.7 (CH), 128.3 (CH), 126.0 (C), 122.7 (CH), 122.2 (C), 120.6 (C), 120.0 (CH), 119.7 (CH), 117.1 (CH), 46.6 (CH_2), 27.4 (CH), 21.1 (CH_3), 16.8 (CH_3).

■ ASSOCIATED CONTENT

Supporting Information

General experimental methods, variable-temperature ^1H NMR spectra of the metal complexes, tables giving Cartesian coordinates and electronic energies for all the calculated species, nonlinear effects, ^1H and ^{13}C NMR spectra and chiral analysis for all new compounds **3**, ORTEP plot and CIF file for the X-ray structure of compound **3ga**. This material is available free of charge via the Internet at http://pubs.acs.org.

■ AUTHOR INFORMATION

Corresponding Author

*E-mail: jose.r.pedro@uv.es; joan.cano@uv.es.

Notes

The authors declare no competing financial interest.

■ ACKNOWLEDGMENTS

Financial support from the Ministerio de Ciencia e Innovación, Gobierno de España and FEDER, European Union (Grant CTQ 2009-13083) and the Generalitat Valenciana (Grants ACOMP/2012/212 and ISIC 2012/001) is acknowledged. C.V. thanks the Generalitat Valenciana for a predoctoral grant

■ REFERENCES

(1) (a) *New Frontiers in Asymmetric Catalysis*; Mikami, K., Lautens, M., Eds.; Wiley: Hoboken, NJ, 2007. (b) *Enantioselective Organocatalysis*; Dalko, P. I., Ed.; Wiley-VCH: Weinheim, 2007. (c) *Comprehensive Asymmetric Catalysis*, Jacobsen, E. N., Pfaltz, A., Yamamoto, H., Eds.; Springer: Berlin, 1999.

(2) (a) Kenji, M. *Chirality* **2011**, *23*, 449−462. (b) Nunez, M. C.; Garcia-Rubino, M. E.; Conejo-Garcia, A.; Cruz-Lopez, O.; Kimatrai, M.; Gallo, M. A.; Espinosa, A.; Campos, J. M. *Curr. Med. Chem.* **2009**, *16*, 2064−2074. (c) Mori, K. *Biorg. Med. Chem.* **2007**, *15*, 7505−7523.

(3) (a) Crassous, J. *Chem. Soc. Rev.* **2009**, *38*, 830−845. (b) Train, C.; Gruselle, M.; Verdaguer, M. *Chem. Soc. Rev.* **2011**, *40*, 3297−3312. (c) Moriuchi, T.; Hirao, T. *Acc. Chem. Res.* **2010**, *43*, 10140−1051.

(4) (a) Lin, P. *Chem. Rev.* **1998**, *98*, 2405−2494. (b) Brunel, J. M. *Chem. Rev.* **2005**, *105*, 857−898.

(5) Ishii, A.; Soloshonok, V. A.; Mikami, K. *J. Org. Chem.* **2000**, *65*, 1597−1599.

(6) For reviews, see: (a) Mikami, K.; Shimizu, M. *Chem. Rev.* **1992**, *92*, 1021−1050. (b) Mikami, K.; Terada, M. In *Lewis Acids in Organic Synthesis*; Yamamoto, H., Ed.; Wiley-VCH: Weinheim, Germany, 2000; Vol. 2, pp 799−847. (c) Chen, Y.; Yekta, S.; Yudin, A. K. *Chem. Rev.* **2003**, *103*, 3155−3211. (d) Ramon, D. J.; Yus, M. *Chem. Rev.* **2006**, *106*, 2126−2208. (e) Yuan, Y.; Ding, K.; Chen, G. In *Acid Catalysis in Modern Organic Synthesis*; Yamamoto, H., Ishihara, K., Eds.; Wiley-VCH: Weinheim, Germany, 2008; Vol. 2, pp 721−823. For recent examples, see: (f) Muramatsu, Y.; Harada, T. *Chem.—Eur. J.* **2008**, *14*, 10560−10563. (g) Yang, F.; Zhao, D.; Lan, J.; Xi, P.; Yang, L.; Xiang, S.; You, J. *Angew. Chem., Int. Ed.* **2008**, *47*, 5646−5649. (h) Bao, H.; Zhou, J.; Wang, Z.; Guo, Y.; You, T.; Ding, K. *J. Am. Chem. Soc.* **2008**, *130*, 10116−10127. (i) Majer, J.; Kwiatkowski, P.; Jurczak, J. *Org. Lett.* **2009**, *11*, 4636−4639. (j) Liu, W. J.; Lv, B. D.; Gong, L. Z. *Angew. Chem., Int. Ed.* **2009**, *48*, 6503−6506. (k) Zhou, S.; Wu, K. H.; Chen, C. A.; Gau, H. M. *J. Org. Chem.* **2009**, *74*, 3500−3505. (l) Yu, R.; Yamashita, Y.; Kobayashi, S. *Adv. Synth. Catal.* **2009**, *351*, 147−152. (m) Biradar, D. B.; Gau, H. M. *Org. Lett.* **2009**, *11*, 499−502. (n) Shono, T.; Harada, T. *Org. Lett.* **2010**, *12*, 5270−5273. (o) Liu, Y.; Da, C. S.; Yu, S. L.; Yin, X. G.; Wang, J. R.; Fan, X. Y.; Li, W. P.; Wang, R. *J. Org. Chem.* **2010**, *75*, 6869−6878. (p) Zhang, Z. G.; Dong, Z. B.; Li, J. S. *Chirality* **2010**, *22*, 820−826. (q) Fan, X. Y.; Yang, Y. X.; Zhuo, F. F.; Yu, S. L.; Li, X.; Guo, Q. P.; Du, Z. X.; Da, C. S. *Chem.—Eur. J.* **2010**, *16*, 7988−7991. (r) Abreu, A. R.; Lourenco, M.; Peral, D.; Rosado, M. T. S.; Eusebio, M. E. S.; Palacios, O.; Bayon, J. C.; Pereira, M. M. *J. Mol. Catal. A: Chem* **2010**, *325*, 91−97. (s) Liu, X.; Wang, P.; Yang, Y.; Wang, P.; Yang, Q. *Chem.—Asian J.* **2010**, *5*, 1232−1239. (t) Hashimoto, T.; Maeda, Y.; Omote, M.; Nakatsu, H.; Maruoka, K. *J. Am. Chem. Soc.* **2010**, *132*, 4076−4077. (u) Majer, J.; Kwiatkowski, P.; Jurczak, J. *Org. Lett.* **2011**, *13*, 5944−5947. (v) Wu, K. H.; Zhou, S.; Chen, C. A.; Yang, M. C.; Chiang, R. T.; Chen, C. R.; Gau, H. M. *Chem. Commun.* **2011**, *47*, 11668−11670. (w) Du, X.; Wang, Q.; He, X.; Peng, R. G.; Zhang, X.; Yu, X. Q. *Tetrahedron: Asymmetry* **2011**, *22*, 1142−1146.

(7) (a) Ihori, Y.; Yamashita, Y.; Ishitani, H.; Kobayashi, S. *J. Am. Chem. Soc.* **2005**, *127*, 15528−15535. (b) Saruhashi, K.; Kobayashi, S. *J. Am. Chem. Soc.* **2006**, *128*, 11232−11235. (c) Mouhtady, O.; Gaspard-Iloughmane, H.; Laporterie, A.; Le Roux, C. *Tetrahedron Lett.* **2006**, *47*, 4125−4128. (d) Kobayashi, S.; Salter, M. M.; Yamazaki, Y.; Yamashita, Y. *Chem.—Asian J.* **2010**, *5*, 493−495.

(8) (a) Yamashita, Y.; Saito, S.; Ishitani, H.; Kobayashi, S. *J. Am. Chem. Soc.* **2003**, *125*, 3793−3798. (b) Gao, B.; Fu, Z.; Yu, Z.; Yu, L.; Huang, Y.; Feng, X. *Tetrahedron* **2005**, *61*, 5822−5830.

(9) (a) Kobayashi, S.; Shimizu, H.; Yamashita, Y.; Ishitani, H.; Kobayashi, J. *J. Am. Chem. Soc.* **2002**, *124*, 13678−13679. (b) Yamashita, Y.; Kobayashi, S. *J. Am. Chem. Soc.* **2004**, *126*, 11279−11282.

(10) Ishitani, H.; Komiyama, S.; Hasegawa, Y.; Kobayashi, S. *J. Am. Chem. Soc.* **2000**, *122*, 762−766.

(11) Gastner, T.; Ishitani, H.; Akiyama, R.; Kobayashi, S. *Angew. Chem., Int. Ed.* **2001**, *40*, 1896−1898.

(12) Yamashita, Y.; Ishitani, H.; Shimizu, H.; Kobayashi, S. *J. Am. Chem. Soc.* **2002**, *124*, 3292−3302.

(13) Seki, K.; Yu, R.; Yamazaki, Y.; Yamashita, Y.; Kobayashi, S. *Chem. Commun.* **2009**, 5722−5724.

(14) Casolari, S.; Cozzi, P. G.; Orioli, P.; Tagliavini, E.; Umani-Ronchi, A. *Chem. Commun.* **1997**, 2123−2124.

(15) (a) Yao, W.; Wang, J. *Org. Lett.* **2003**, *5*, 1527−1530. (b) Kobayashi, J.; Nakamura, M.; Mori, Y.; Yamashita, Y.; Kobayashi, S. *J. Am. Chem. Soc.* **2004**, *126*, 9192−9193.

(16) (a) Schneider, C.; Hansch, M. *Synlett* **2003**, 837−840. (b) Schneider, C.; Hansch, M.; Sreekumar, P. *Tetrahedron: Asymmetry* **2006**, *17*, 2738−2742.

(17) Kobayashi, S.; Yakazi, R.; Seki, K.; Ueno, M. *Tetrahedron* **2007**, *63*, 8425−8429.

(18) (a) Blay, G.; Fernández, I.; Pedro, J. R.; Vila, C. *Org. Lett.* **2007**, *9*, 2601−2604. (b) Blay, G.; Fernández, I.; Pedro, J. R.; Vila, C. *Tetrahedron Lett.* **2007**, *48*, 6731−6734. (c) Blay, G.; Fernández, I.; Muñoz, M. C.; Pedro, J. R.; Vila, C. *Chem.—Eur. J.* **2010**, *16*, 9117−9122.

(19) (a) Katsuki, T.; Sharpless, K. B. *J. Am. Chem. Soc.* **1980**, *102*, 5974−5776. (b) Johnson, R. A.; Sharpless, K. B. In *Catalytic Asymmetric Synthesis*; Ojima, I., Ed.; VCH: New York, 1993. (c) Lappert, M. F. In *Comprehensive Organometallic Chemistry 2*; Abel, E. W., Stone, F. G. A., Wilkinson, G., Eds.; Pergamon: Oxford, 1995; Vol. 4, pp 213−632.

(20) (a) Boyle, T. L; Barnes, D. L.; Heppert, J. A. *Organometallics* **1992**, *11*, 1112−1126. (b) Boyle, T. J.; Eilerts, N. W.; Heppert, J. A.; Takusagawa, F. *Organometallics* **1994**, *13*, 2218−2229.

(21) Tang, H. Z.; Boyle, P. D.; Novak, B. M. *J. Am. Chem. Soc.* **2005**, *127*, 2136−2142.

(22) Yamashita, Y.; Ishitani, H.; Shimizu, H.; Kobayashi, S. *J. Am. Chem. Soc.* **2002**, *124*, 3292−3302.
(23) It has been observed that the enantioselectivities obtained in reactions catalyzed by complexes of group IV metals with BINOL-derived ligands is altered by the addition of protic solvents, which modifies the structure of the catalyst. See: Blay, G.; Fernández, I.; Monleon, A.; Muñoz, M. C.; Pedro, J. R.; Vila, C. *Adv. Synth. Catal.* **2009**, *351*, 2433−2440 and ref 22.
(24) The presence of released alcohol in the titanium(IV)−BINOL catalyzed allylation of ketones has been shown to be essential to obtain good enantioselectivities, although its role has not been clarified. See: (a) Kim, J. G.; Waltz, K. M.; Garcia, I. F.; Kwiatkowski, D.; Walsh, P. J. *J. Am. Chem. Soc.* **2004**, *126*, 12580−12585. (b) Waltz, K. M.; Gavenonis, J.; Walsh, P. J. *Angew. Chem., Int. Ed.* **2002**, *41*, 3697−3699.
(25) (a) Becke, A. D. *Phys. Rev. A* **1988**, *38*, 3098−3103. (b) Lee, C. T.; Yang, W. T.; Parr, R. G. *Phys. Rev. B* **1988**, *37*, 785−789. (c) Becke, A. D. *J. Chem. Phys.* **1993**, *98*, 5648−5652. (d) Bacskay, G. B. *Chem. Phys.* **1981**, *61*, 385−404. (e) Frisch, M. J.; Trucks, G. W.; Schlegel, H. B.; Scuseria, G. E.; Robb, M. A.; Cheeseman, J. R.; Scalmani, G.; Barone, V.; Mennucci, B.; Petersson, G. A.; Nakatsuji, H.; Caricato, M.; Li, X.; Hratchian, H. P.; Izmaylov, A. F.; Bloino, J.; Zheng, G.; Sonnenberg, J. L.; Hada, M.; Ehara, M.; Toyota, K.; Fukuda, R.; Hasegawa, J.; Ishida, M.; Nakajima, T.; Honda, Y.; Kitao, O.; Nakai, H.; Vreven, T.; Montgomery, J. A., Jr.; Peralta, J. E.; Ogliaro, F.; Bearpark, M.; Heyd, J. J.; Brothers, E.; Kudin, K. N.; Staroverov, V. N.; Kobayashi, R.; Normand, J. ; Raghavachari, K.; Rendell, A.; Burant, J. C.; Iyengar, S. S.; Tomasi, J.; Cossi, M.; Rega, N.; Millam, J. M.; Klene, M.; Knox, J. E.; Cross, J. B.; Bakken, V.; Adamo, C.; Jaramillo, J.; Gomperts, R.; Stratmann, R. E.; Yazyev, O. ; Austin, A. J.; Cammi, R.; Pomelli, C.; Ochterski, J. W.; Martin, R. L.; Morokuma, K.; Zakrzewski, V. G.; Voth, G. A.; Salvador, P.; Dannenberg, J. J.; Dapprich, S.; Daniels, A. D.; Farkas, Ö.; Foresman, J. B.; Ortiz, J. V.; Cioslowski, J.; Fox, D. J. *Gaussian 09*, Revision A.2; Gaussian, Inc.: Wallingford, CT, 2009.
(26) Schäfer, A.; Horn, H.; Ahlrichs, R. *J. Chem. Phys.* **1992**, *97*, 2571−2577.
(27) Dunning, T. H. Jr.; Hay, P. J. In *Modern Theoretical Chemistry*; Schaefer, H. F. III, Ed.; Plenum: New York, 1976; Vol. 3, pp 1−28.
(28) (a) Hay, P. J.; Wadt, W. R. *J. Chem. Phys.* **1985**, *82*, 270−83. (b) Hay, P. J.; Wadt, W. R. *J. Chem. Phys.* **1985**, *82*, 299−310. (c) Wadt, W. R.; Hay, P. J. *J. Chem. Phys.* **1985**, *82*, 284−298.
(29) (a) Keith, T. A.; Bader, R. F. W. *Chem. Phys. Lett.* **1992**, *194*, 1−8. (b) Keith, T. A.; Bader, R. F. W. *Chem. Phys. Lett.* **1993**, *210*, 223−231. (c) Cheeseman, J. R.; Trucks, G. W.; Keith, T. A.; Frisch, M. J. *J. Chem. Phys.* **1996**, *104*, 5497−5509.
(30) (a) London, F. *J. Phys. Radium* **1937**, *8*, 397−409. (b) McWeeny, R. *Phys. Rev.* **1962**, *126*, 1028−1034. (c) Ditchfield, R. *Mol. Phys.* **1974**, *27*, 789−807. (d) Wolinski, K.; Hilton, J. F.; Pulay, P. *J. Am. Chem. Soc.* **1990**, *112*, 8251−8260.
(31) (a) Nishio, M.; Umezawa, Y.; Hirota, M.; Takeuchi, Y. *Tetrahedron* **1995**, *51*, 8665−8701. (b) Meot-Ner, M. *Chem. Rev.* **2005**, *105*, 213−284. (c) Calhorda, M. K. *Chem. Commun.* **2000**, 801−809. (d) Grabowski, S. J. *Chem. Rev.* **2011**, *111*, 2597−2625.
(32) Although the cause of this different behavior is not completely clear, it may be due to the easier coordination of the enone to a pentacoordinated Zr(IV) atom with an approximate binding angle of 120° compared to the tetracoordinated Ti(IV) with an approximate binding angle of 109°.
(33) Similar experiments carried out with racemic 3,3′-Br_2−BINOL and $Ti(O^tBu)_4$ showed ^1H NMR spectrum identical to that obtained from optically pure (*R*)-3,3′-Br_2BINOL and $Ti(O^tBu)_4$. On the other hand, the low activity and enantioselectivity of the (*R*)-L-$Ti(O^tBu)_4$ prevented NLE studies with this complex. Therefore, the influence of the enantiomeric excess of the catalyst on the reaction rate was considered. A measure of the conversion of the starting materials into the Friedel−Crafts product after 22 h (^1H NMR) carried out with catalysts prepared from (*R*)-3,3′-Br_2−BINOL of different ee and $Ti(O^tBu)_4$ did not show appreciable differences on the reaction rate: 37% (ee_{cat} = 100%), 35% (ee_{cat} = 60%), 39% (ee_{cat} = 30%), 34% (ee_{cat} = 0%).
(34) These experiments were proposed by one of the referees who suggested that the little change in the NMR spectrum after addition of the enone may be due to a very small equilibrium constant for coordination of the enone and a fast exchange and not to the maintenance of the dimeric complex.
(35) For reviews on bifunctional catalysts, see: (a) Shibasaki, M.; Sasai, H.; Arai, T. *Angew. Chem., Int. Ed. Engl.* **1997**, *36*, 1236−1256. (b) Shibasaki, M.; Yoshikawa, N. *Chem. Rev.* **2002**, *102*, 2187−2210. (c) Shibasaki, M.; Matsunaga, S. *Chem. Soc. Rev.* **2006**, *35*, 269−279.
(36) (a) Bandini, M.; Fagioli, M.; Garavelli, M.; Melloni, A.; Trigari, V.; Umani-Ronchi, A. *J. Org. Chem.* **2004**, *69*, 7511−7518. (b) Bandini, M.; Fagioli, M.; Melchiorre, P.; Melloni, A.; Umani-Ronchi, A. *Tetrahedron Lett.* **2003**, *44*, 5843−5846.
(37) CCDC 861026 contains the supplementary crystallographic data for this paper. These data can be obtained free of charge from The Cambridge Crystallographic Data Centre via www.ccdc.cam.ac.uk/data_request/cif.
(38) In spite of the steric congestion around of the Zr atoms, the metal contains an open site to which the enone might bind. At the present time, the issue of the coordination number (5 or 6) of the catalyst−substrate complex remains unresolved.
(39) For general experimental procedures, see ref 18a or the Supporting Information.